CS$_2$ capture in the ionic liquid 1-alkyl–3-methylimidazolium acetate: reaction mechanism and free energetics

CS$_2$ capture in the ionic liquid 1-alkyl-3-methylimidazolium acetate: reaction mechanism and free energetics

Fangyong Yan,[1] Ryohei Kakuchi,[2] Kenji Takahashi[3] and Hyung J. Kim[1]*

[1]Department of Chemistry, Carnegie Mellon University, Pittsburgh, PA 15213, USA
[2]Division of Molecular Science, Graduate School of Science and Technology, Gunma University, 1-5-1 Tenjin-cho, Kiryu 376-8515, Gunma, Japan.
[3]Institue of Science and Engineering, Kanazawa University, Kanazawa 920-1192, Japan

Abstract

Reaction pathways for CS$_2$ and COS in the ionic liquid, 1-ethyl-3-methylimidazolium (EMI$^+$) acetate (OAc$^-$), are studied using the *ab initio* self-consistent reaction field theory (SCRF) and molecular dynamics (MD) computer simulations. It is found that while CS$_2$ converts to COS nearly at the 100% level through S/O exchange with acetate, both conversion and capture processes are kinetically possible for COS, yielding CO$_2$/thioacetate and 1-ethyl-3-methylimidazole-2-thiocarboxylate (EMI-COS)/acetic acid as reaction products, respectively. These findings are in excellent agreement with recent experimental observations in the closely related 1-butyl-3-methylimidazolium acetate (BMI$^+$OAc$^-$) ionic liquid system. Constrained *ab initio* MD indicates that the capture reaction of COS (and CS$_2$ if allowed) proceeds in a concerted fashion; *viz.*, proton transfer from EMI$^+$ to OAc$^-$ and carboxylation of EMI$^+$ by COS (and CS$_2$) occur concurrently, analogous to the concerted pathway proposed recently for CO$_2$ capture in the imidazolium acetate ionic liquid family. As N-heterocyclic carbene (NHC) is not required, the concerted mechanism is fully consistent with the experimental fact that NHC has not been detected directly in this ionic liquid family. Computational analysis further predicts that if NHC would be present in the ionic liquid, it would react with CS$_2$ and produce 1-ethyl-3-imidazole-2-dithiocarboxylate, prior to the conversion of CS$_2$ to COS. Since such a dithiocarboxylate compound was not detected experimentally, the present analysis lends support to the view that NHC is not formed in the pure imidazolium acetate ionic liquid family.

Introduction

Ionic liquids (ILs)[1-4] are a class of organic salts that have melting points generally lower than 100ºC. ILs have many desirable properties, including low volatility, low flammability, good thermal stability, high intrinsic ion concentration, and wide electrochemical window. ILs are sometimes referred to as designer solvents because these properties can be tuned for specific tasks through judicious choice and combination of cations and anions. As such, ILs have evolved from a novel subject of academic curiosity to an exciting class of materials that can enable green technology[5-10] in a broad range of applications[1-30] in synthesis, catalysis, and separation, including areas as diverse as CO$_2$ capture,[19-21] diesel fuel desulfurization[22,23] and biomass processing,[24-30] and in

electrochemical processes as electrolytes, such as in energy storage and conversion devices.[31-35]

In the last 10-15 years, there has been an intensive effort to understand physicochemical properties of ILs. Among others, ILs based on imidazolium cations (Figure 1a) have received probably the most extensive attention partly due to ease of customization and control of their properties and partly due to their important role in the development of ILs. Nevertheless, molecular details of chemical processes in these ILs are still not well understood. A good example is mechanisms of various reactions, such as trapping reactions,[36] benzoin condensation,[37-40] CO_2 capture,[41-49] *etc*., in the imidazolium acetate IL family, which are the subject of much controversy recently. This state of affairs is largely due to differing and confusing views on N-heterocyclic carbene (NHC) (Figure 1b)—*viz*., whether it would be formed in neat imidazolium acetate ILs and what roles it would play if it would be indeed formed. To be specific, despite the lack of direct experimental evidence, it has been generally believed that NHC is produced via transfer of acidic proton, denoted as H2 hereafter, from the C2 position of imidazolium to one of the oxygen atoms of acetate (see Figure 2a for atom labels). NHC thus formed is then assumed to play an active role in most of the aforementioned reactions in this IL family ("carbene mechanism").

However, recent quantum chemistry calculations by Yan *et al*., using the self-consistent reaction field theory (SCRF) method, indicated that the formation of carbene from imidazolium cations becomes totally unfavorable energetically in polar environments, such as pure imidazolium acetate.[49] The solvation-induced destabilization of the product state, NHC + acetic acid, compared to the ion pair reactant state, makes the product state unstable in solution.[49] Furthermore, *ab initio* MD analysis with the constrained dynamics method suggests that in the case of CO_2 capture, the reaction proceeds in a concerted manner, completely bypassing NHC; specifically, proton transfer from imiazolium to acetate and carboxylation of imidazolium by CO_2 occur *concurrently*.[49] Combined experimental and theoretical investigation of transesterification of 2-phenylethyl alcohol with isopropenyl acetate also suggests the absence of free NHC in the imidazolium acetate IL family.[50] Interestingly, Welton and coworkers found very recently that benzoin condensation reaction in EMI^+OAc^- did not exhibit any kinetic isotope effect (KIE) when imidazolium was deuterated.[40] They interpreted this result as direct evidence for the "pre-formation"—*i.e.*, existence—of NHC in EMI^+OAc^-, as a concerted mechanism like the one proposed for CO_2 capture[49] must yield a significant isotope effect. Though care is needed in the interpretation of KIE,[51] we have a different view on their finding; *viz*., the step involving proton transfer from imidazolium to acetate, whether concerted or not, is not rate-limiting in benzoin condensation. Thus while NHC is an important reaction intermediate in organocatalysis[52] and organometallic catalysis,[53] it is a measure of the very open for discussion character of NHC formation and participation, or lack thereof, in chemical processes in imidazolium acetate that different mechanisms and interpretations of kinetic measurements in this IL family have been proposed, continuing to the present. To avoid confusion, it should be mentioned that NHC can be formed in other imidazolium-based ILs containing sufficiently basic anions, such as hydroxide and hydride.[54,55]
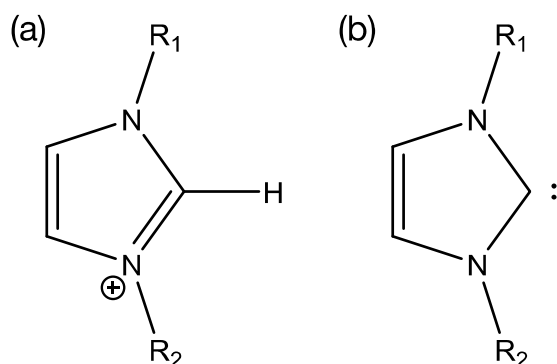
Figure 1. (a) Imidazolium cation and (b) N-heterocyclic carbene.

In this article, we extend the analysis of ref 49 to study CS_2 capture in imidazolium acetate.[56-58] Experimentally, a mixture of CS_2 with the ionic liquid, 1-butyl-3-methylimidazolium acetate (BMI^+OAc^-), was found to yield as reaction products both 1-butyl-3-methylimidazole-2-thiocarboxylate and -2-carboxylate, BMI-COS and BMI-CO$_2$, but not 1-butyl-3-methylimidazole-2-dithiocarboxylate, BMI-CS$_2$.[56,57] This occurs despite the fact that COS and CO_2 were not present originally in the system. This intriguing result was explained by S/O exchange with acetate, which converts CS_2 to COS and some of COS thus generated to CO_2, prior to the capture reaction. DFT calculations with B3LYP indicated that the activation energies for the conversion of CS_2 to COS and COS to CO_2 are, respectively, 24.5 and 23.9 kcal/mol in the presence of a pair of BMI^+ and OAc^- ions in the gas-phase though different functionals/basis-sets yield somewhat different results.[57,58] The capture of CS_2, COS and CO_2 by (transient) 1-butyl-3-methylimidazole-2-ylidene carbene was also examined in refs 57 and 58. While these analyses offer valuable insights, they do not shed much light on the actual solution-phase processes. Herein, we present the results of *ab initio* SCRF calculations and *ab initio* MD simulations to obtain molecular details for CS_2 (and COS) capture in EMI^+OAc^- and to gain further insight into issues surrounding NHC in the imidazolium acetate IL family.

Models and Methods

Ab initio calculations were performed using GAUSSIAN-09 (G09RevA.02) program.[59] DFT calculations were carried out at the B3LYP level[60,61] with the unrestricted UB3LYP functional for CS_2-to-COS and COS-to-CO_2 conversions via S/O exchange with acetate, and for CO_2/COS/CS_2 capture reactions via 1-ethyl-3-methylimida-2-ylidene (EMI) carbene. In all calculations, the MQZVP (modified QZVP)[62] basis set was used for sulfur while the 6-31+G(d,p) basis set was employed for all other atom types. The dielectric constant of 15.13, corresponding to 1-pentanol, was used for the continuum solvent in the SCRF calculations. Since the dielectric constant of many ILs is in the range $\varepsilon \sim 10–16$, the solvation effect, though implicit at the continuum level, on reaction free energetics in EMI^+OAc^- is accounted for in our *ab initio* SCRF calculations, in contrast to the earlier studies in BMI^+OAc^-.[57,58]

In addition to electronic structure calculations in the continuum phase, we have performed *ab initio* MD simulations using the CP2K program.[63] Four different systems were considered: (i) 12 pairs of EMI^+ and OAc^- ions, *i.e.*, 12 ion pairs (IPs), (ii) 12 IPs and 6 CS_2 molecules, (iii) 12 IPs and 6 COS molecules, and (iv) 12 IPs and 6 CS_2 molecules plus 1 NHC molecule, EMI. These systems will be denoted as 12:0, 12:6CS_2 and 12:6COS, 12:6CS_2:1EMI, respectively. To obtain the initial configurations needed for the *ab initio* simulations, we first conducted classical MD simulations in the isothermal-isobaric ensemble at 298 K and 1 bar using GROMACS 4.6.[64] The force field parameters for EMI^+ and OAc^- were taken from refs 65 and 66. The partial charges and the van der Waals parameters of CS_2 were taken from ref 67 and ref 68, respectively, while the force field parameters of ref 69 were employed for COS. For both CS_2 and COS, a rigid linear geometry was used. Partial charges of EMI carbene were obtained by performing charge density population analysis using the CHELPG method[70] on the optimized geometry determined via DFT with the B3LYP functional in the 6-311++G(d,p) basis set. This is consistent with the determination of partial charges of the EMI^+ cation in ref 65, employed in our study. Other force field parameters of EMI were assumed be the same as those of EMI^+.

For both classical and *ab initio* MD simulations, we employed the same procedure as in ref 49. Briefly, for classical MD, the system was equilibrated for 6 ns, followed by a 24 ns production run, from which average density was computed. A configuration whose density is arbitrarily close to the average density of the isothermal–isobaric ensemble was chosen from this trajectory and used as the starting configuration for *ab initio* MD. The BLYP functional[61,71] with the DFT-D2 van der Waals correction[72] and the DZVP-GTH-BLYP basis set with Goedecker, Teter and Hutter (GTH) pseudopotentials[73] were employed for *ab initio* simulations. Geometry relaxation of the initial configuration was performed until the forces on atoms became smaller than 0.02 eV $Å^{-1}$ in magnitude. Once the geometry was optimized, *ab initio* MD was carried out in the canonical ensemble at 298 K, using the Nosé–Hoover thermostat[74,75] and a time step of 0.5 fs with periodic, cubic boundary conditions applied. We simulated two trajectories, each with 5 ps equilibration followed by a 50-60 ps production run, from which averages were computed.

To investigate the potential of mean force *w(r)*,

$$w(r) \ = \ -k_B T \ \ln g(r) \ ; \qquad f(r) \ = \ - \partial w(r) / \partial r \qquad (1)$$

for capture reactions, we conducted constrained *ab initio* MD by employing the distance *r* between C2 of EMI^+/EMI (Figures 1 and 2a) and the carbon atom, Cc, of CS_2/COS as the reaction coordinate. In eq 1, $\cdot (r)$ and *f(r)* are, respectively, the radial distribution function and the mean force between C2 and Cc, *T* is the system temperature and k_B is Boltzmann's constant. We selected a configuration with the Cc–C2 distance of 4.0 Å from the unconstrained *ab initio* MD results and slowly changed the *r* value to a target Cc–C2 distance at the rate of 0.001 Å per fs. The target distance ranged between 1.5 and 4.0 Å in the present study. The system thus prepared was equilibrated for 5 ps with the Cc–C2 distance frozen, followed by a 5 ps production simulation from which mean force *f(r)* in eq 1 was computed. For systems

near the transition state, *i.e.*, the Cc–C2 distance is close to the separation, at which *f(r)* between Cc and C2 varies rapidly with proton transfer, the production run was 15-30 ps.

Results and Discussion

CS_2-to-COS and COS-to-CO_2 conversions via S/O exchange with OAc^-

We begin with the *ab initio* results for S/O exchange between CS_2/COS and OAc^- in Figures 2-4. As noted above, our systems are similar to those studied in refs 57 and 58 except that the cationic species we considered is EMI^+ and the solvation effect, though at the continuum level, is incorporated into our calculations.
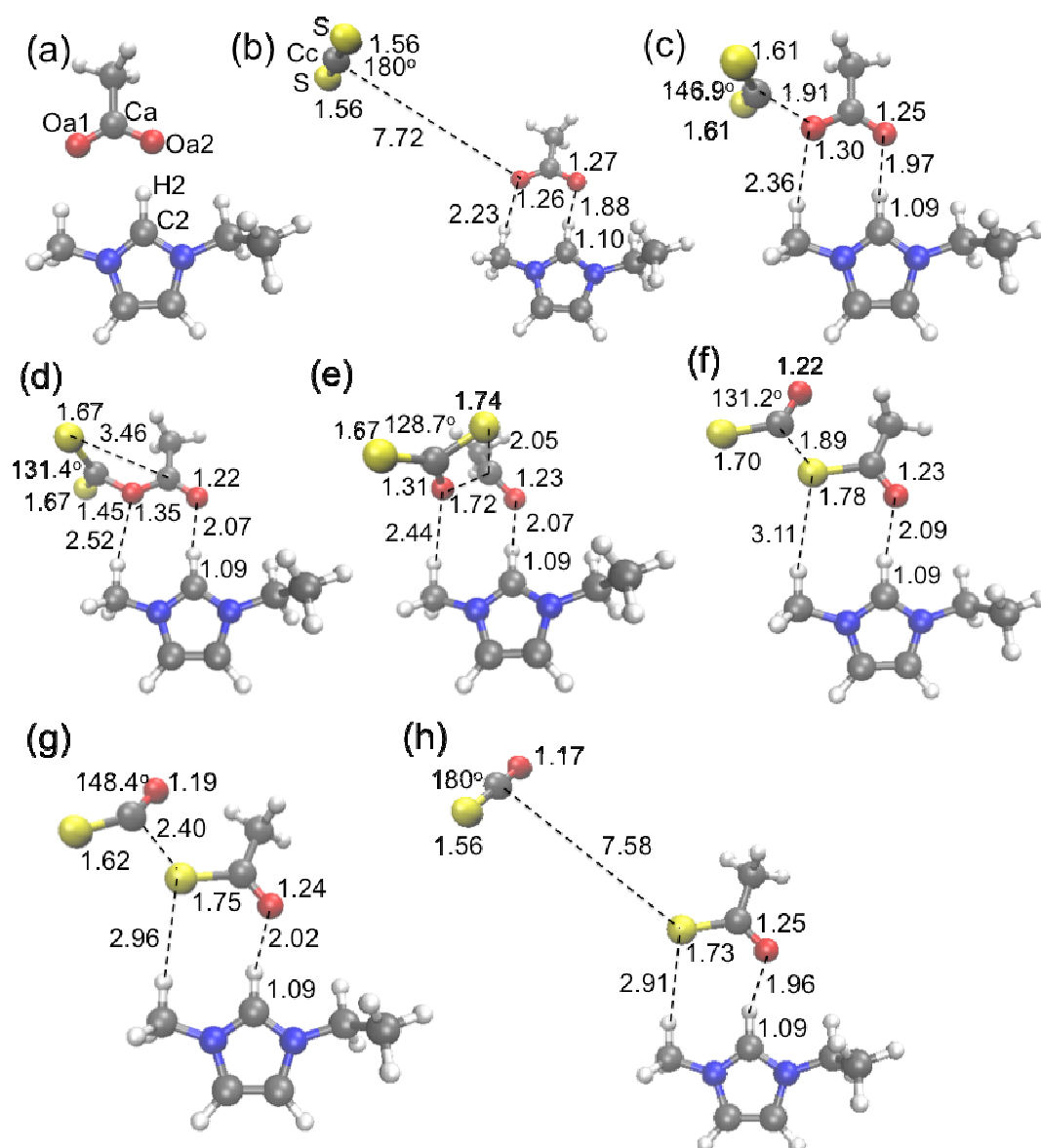
Figure 2. CS_2 to COS conversion in the presence of an EMI^+-OAc^- ion pair in the continuum phase. The atom labels and the structures of the reactant, product and transition states as well as those of the reaction intermediates are displayed: (a) Atom labels; (b) Reac; (c) TS1; (d) Int1; (e) TS2; (f) Int2; (g) TS3; (h) Prod. Here Reac and Prod are the reactant and product states of the exchange reaction, while TS1, TS2 and TS 3 are transition states for conversion to the intermediate states, Int1 and Int2, and the product state Prod, respectively. Distance is measured in units of Å.

IRC (intrinsic reaction coordinate) calculation results for the conversion of CS_2 to COS in the dielectric continuum ($\varepsilon = 15.13$) obtained via DFT are presented in Figure 2 with atom labels shown in Figure 2a. The overall reaction proceeds in three steps: complexation of CS_2 and OAc^-, S/O exchange between the two, and de-complexation of the products COS and CH_3COS^- (SAc^-). The long distance of 7.72 Å between Cc of CS_2 and Oa of OAc^- in Figure 2b clearly indicates that there are no significant interactions between CS_2 and OAc^- in the reactant state, Reac, prior to complexation. The transition state TS1 for complexation in Figure 2c is characterized by the dramatically reduced Cc-Oa distance of 1.91 Å and an activation (free) energy of 17.0 kcal/mol compared to Reac. The resulting CS_2-OAc^- complex in the intermediate state Int1 in Figure 2d exhibits considerable geometry relaxation, including the elongation of the Ca-Oa1 bond from 1.30 Å (TS1) to 1.35 Å (Int1) and shortening of the Ca-Oa2 bond from 1.25 Å (TS1) to 1.22 Å (Int1) in addition to a further reduction of Cc-Oa distance to 1.45 Å. DFT predicts that Int1 is higher in energy than Reac by 11.7 kcal/mol. The transition state TS2 for the actual S/O exchange step that yields COS and SAc^- is displayed in Figure 2e. Activation of Int1 to TS2 involves a significant inner-sphere reorganization, *viz.*, decrease of the S-Ca distance from 3.46 Å to 2.05 Å, increase of the Ca-Oa1 bond length from 1.35 Å to 1.72 Å and decrease of the Cc-Oa1 distance from 1.45 Å to 1.31 Å. As pointed out in ref 58, it is a bi-radical state with an overall spin singlet. As such, TS2 is higher in free energy than Int1 by 9.7 kcal/mol and Reac by 21.4 kcal/mol. The decrease of the Cc-Oa1 from 1.31 Å to 1.22 Å and the S-Ca distance from 2.05 Å to 1.89 Å for the second intermediate state Int2 (Figure 2f) indicates the formation of a complex comprising a COS molecule and an SAc^- anion, *i.e.,* completion of the S/O exchange. Decomplexation of this complex is also an activated process with the relatively low transition state TS3 (Figure 2g), compared to TS1 and TS2. Resulting final products are solvated COS and an EMI^+-SAc^- ion pair. Our *ab initio* SCRF results indicate that the activation to TS2 with the overall barrier height of 21.4 kcal/mol is rate-limiting for CS_2 to COS conversion. This compares well with the gas-phase DFT results.[57,58]

The reaction pathway for the conversion of COS to CO_2 is shown in Figure 3. Its qualitative aspects are essentially the same as those of the CS_2-to-COS conversion in Figure 2. The overall conversion reaction consists of the same three steps, complexation, S/O exchange and decomplexation, and the S/O exchage step is rate-limiting. The activation free energy for the conversion of COS to CO_2 is 20.4 kcal/mol, which is 1 kcal/mol lower than that of CS_2 to COS. For convenience, the SCRF results for the reactant, product, transition and intermediate states for the two conversion processes are summarized in Figure 4.
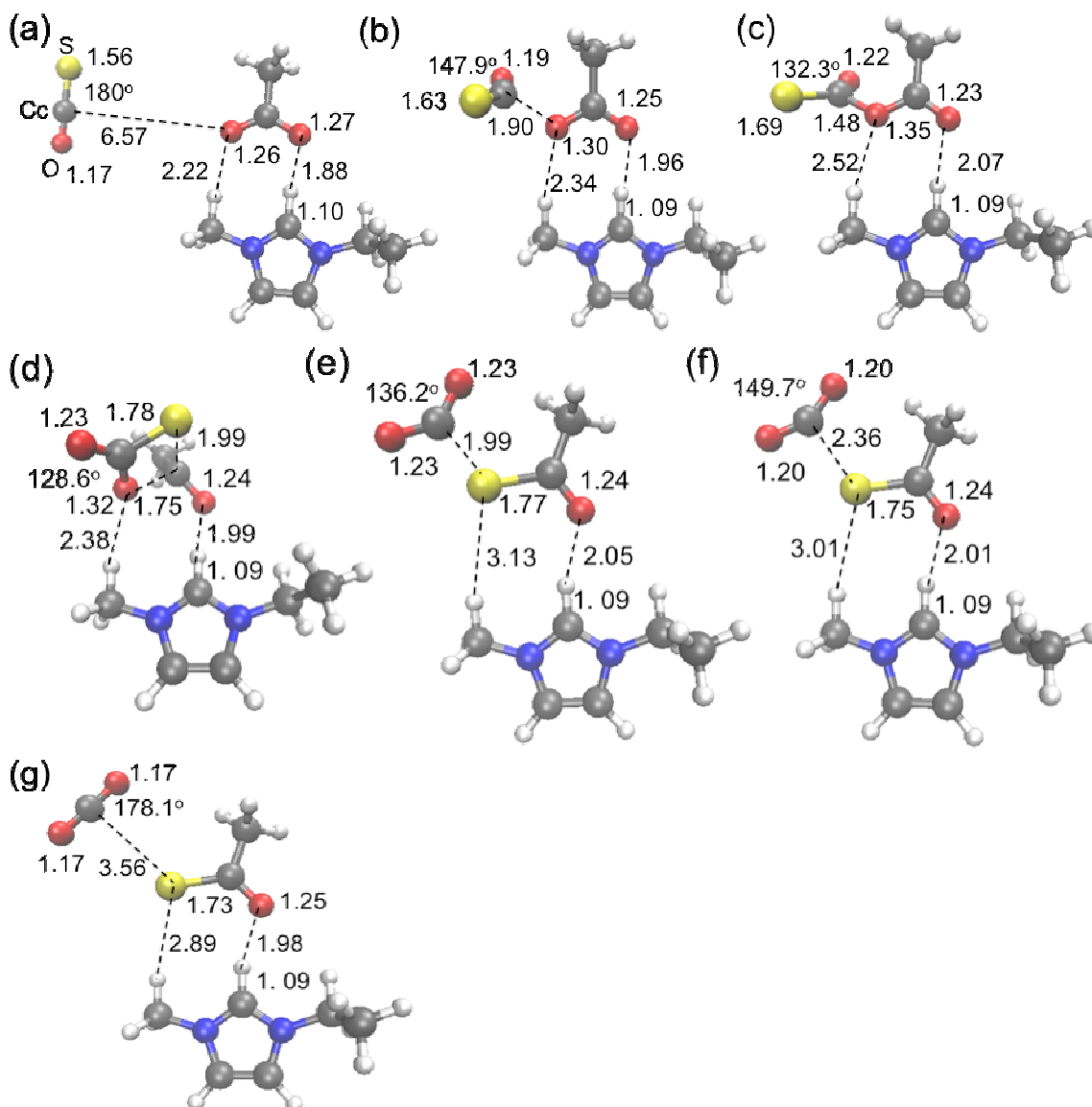
Figure 3. COS to CO$_2$ conversion in the presence of an EMI$^+$-OAc$^-$ ion pair in the continuum phase. (a) Reac; (b) TS1; (c) Int1; (d) TS2; (e) Int2; (f) TS3; (g) Prod.

Before we turn to direct capture of CS$_2$/COS/CO$_2$ by NHC, we briefly pause here for perspective on the SCRF results obtained with ε = 15.13 above. According to many experimental and computational studies,[77] the effective polarity of ILs gauged by solvatochromic shifts, *i.e.*, capability of solvating dipolar solutes, is comparable to that of highly polar solvents even though the typical dielectric constant of ILs ($\varepsilon \sim$ 10–16) is not that high as noted above. This is due to strong stabilization of dipolar solutes in ILs through Coulomb interactions with ILs' free charges, *viz.*, cations and anions that can

reorganize around the solutes independently of each other unlike bound charges of normal solvents.[77,78] To gain insight into how this aspect might influence the continuum solvent results, we performed SCRF calculations for COS-to-CO$_2$ conversion in ethanol (ε = 24.85), whose effective polarity is comparable to that of imidazolium-based ionic liquids. Comparison of the ethanol vis-à-vis 1-pentanol results shows that the difference in free energy along IRC between the two solvents is less than 0.3 kcal/mol (Table S1 in Supplementary Information). Thus an increase in the dielectric constant over the 1-pentanol value does not introduce any significant changes in the SCRF results. From molecular perspective, since the contact ion-pair nature of the cation and anion of the S/O exchange systems we studied remains largely unchanged throughout the entire reaction (*cf.* Figures 2 and 3), the effect of the aforementioned solvation stabilization enhancement arising from IL free charge rearrangements would not vary substantially along IRC. Therefore the dielectric continuum description provides a reasonable framework to capture the solvation effect on CS$_2$-to-COS and COS-to-CO$_2$ conversions in EMI$^+$OAc$^-$.
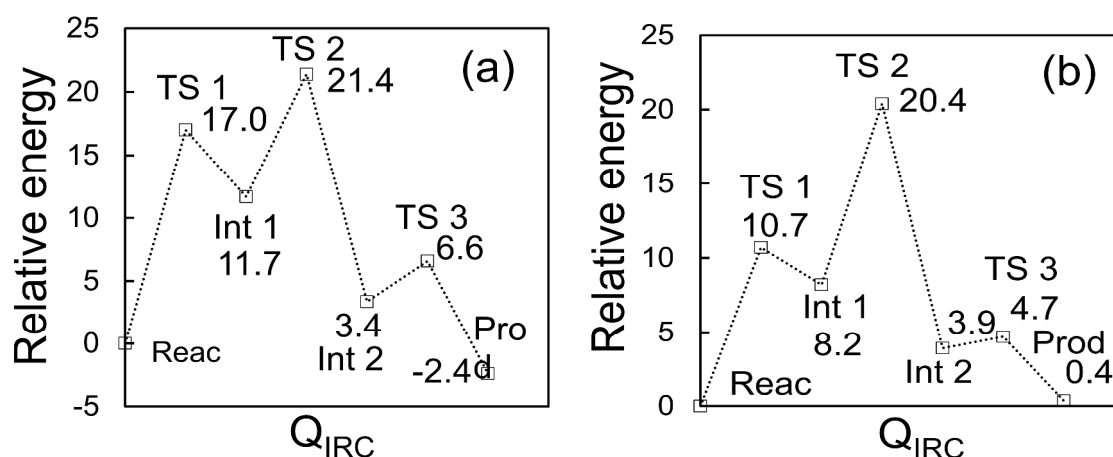

Figure 4. SCRF results for conversion of CS$_2$/COS to COS/CO$_2$ via S/O exchange with OAc$^-$ of an EMI$^+$-OAc$^-$ ion pair in the dielectric continuum: (a) CS$_2$ to COS; (b) COS to CO$_2$. Energies are measured in units of kcal/mol. All results are zero-point energy corrected.

CS$_2$/COS/CO$_2$ capture by EMI carbene

Previous *ab initio* study by Yan *et al.*[49] showed that the electrically-neutral EMI carbene paired with HOAc is thermodynamically unstable except in a non-polar environment (*e.g.*, gas phase) due to solvation destabilization. This indicates that proton transfer from EMI$^+$ to OAc$^-$ does not occur and thus NHC is not formed in the imidazolium acetate IL family, in concert with experimental observations. As will be discussed below, our analysis will further support this view. Nonetheless, the formation of NHC can be induced, for example, by adding a strong base to the reaction system though it may not be produced spontaneously in neat imidazolium acetate. In view of this possibility, we consider here an interesting question, "what roles would NHC play if it would be present in the reaction system?" To this end, we performed DFT and

MP2 calculations for direct capture of CS_2, COS and CO_2 by EMI carbene. The results are presented in Table 1 and Figure 5.

Ab initio calculations predict that all three capture reactions are activated processes both in the gas phase and in solution. The DFT result for barrier height for CS_2 capture in the continuum solvent with $\varepsilon = 15.13$ is 13.3 kcal/mol, which is higher than that for COS or CO_2 by ~6 kcal/mol (Table 1). For all three capture processes, the activation barrier changes by $\leq$ ~0.1 kcal/mol when the dielectric constant is raised from 15.13 to the ethanol value 24.85. In the gas phase, the corresponding barrier for CS_2 capture is 12.9 kcal/mol, ~5 kcal/mol higher than COS or CO_2 capture. Though similar to DFT results, MP2 predicts that the activation free energy for CO_2 capture is lower than that for COS by ~5 kcal/mol. All three reactions are strongly exothermic, indicating that their products are very stable, especially, in solution. This is due to solvation stabilization of highly dipolar product states with respect to weakly dipolar reactant states (see Table S2 for dipole moments of the reactant and product states). For both the transition and product states, C2-Cc distance, r, increases as sulfur atoms of CS_2 are replaced by oxygen atoms; for example, the C2-Cc bond length of the product state is 1.49, 1.52 and 1.54 Å for EMI-CS_2, EMI-COS and EMI-CO_2, respectively (Figure 5bcd). This trend is attributed to high electronegativity of O. To be specific, more electronegative oxygen withdraws electron density from the C2-Cc bonding region better than sulfur and thus makes the C2-Cc "bond" weaker, *i.e.,* longer. We also notice that the orientation of the carboxylate group with respect to the imidazolium ring becomes more twisted with the substitution of O by S. This is primarily due to the increasing steric hindrance with the substitution.

Table 1 Free energetics for capture of CS_2, COS and CO_2 by EMI carbene[1),2)]

System	Reactant	Transition state	Product
EMI-CS_2 (gas phase)	0.0	12.9 (10.9)	-14.6 (-20.9)
EMI-COS (gas phase)	0.0	7.5 (7.9)	-7.6 (-10.4)
EMI-CO_2 (gas phase)	0.0	8.0 (3.4)	-6.6 (-7.0)
EMI-CS_2 (continuum)	0.0	13.3 (11.6)	-21.4 (-28.7)
EMI-COS (continuum)	0.0	7.4 (8.6)	-17.4 (-20.5)
EMI-CO_2 (continuum)	0.0	7.2 (3.3)	-19.2 (-19.3)

[1)] Energy units: kcal/mol
[2)] MP2 results are given in parentheses.

One of the key results of our analysis here is that the activation free energy for the direct capture of CS_2 by EMI carbene (13.3 kcal/mol) is much lower than that for the conversion of CS_2 to COS via S/O exchange with acetate (21.4 kcal/mol). This means that if EMI carbene would be indeed present in EMI^+OAc^-, it would readily react with and capture CS_2, thereby producing 1-ethyl-3-methylimidazole-2-dithiocarboxylate, EMI-CS_2, *prior to* the conversion of CS_2 to COS in the mixture of CS_2 and EMI^+OAc^-. The fact that a similar product, BMI-CS_2, was not observed experimentally in the mixture of CS_2 and BMI^+OAc^-, combined with our results here for direct capture, provides further evidence that NHC is not pre-formed in pure imidazolium acetate. With this in mind, we proceed to *ab initio* MD simulations, in which the solvation effect is included at the first principles molecular level.
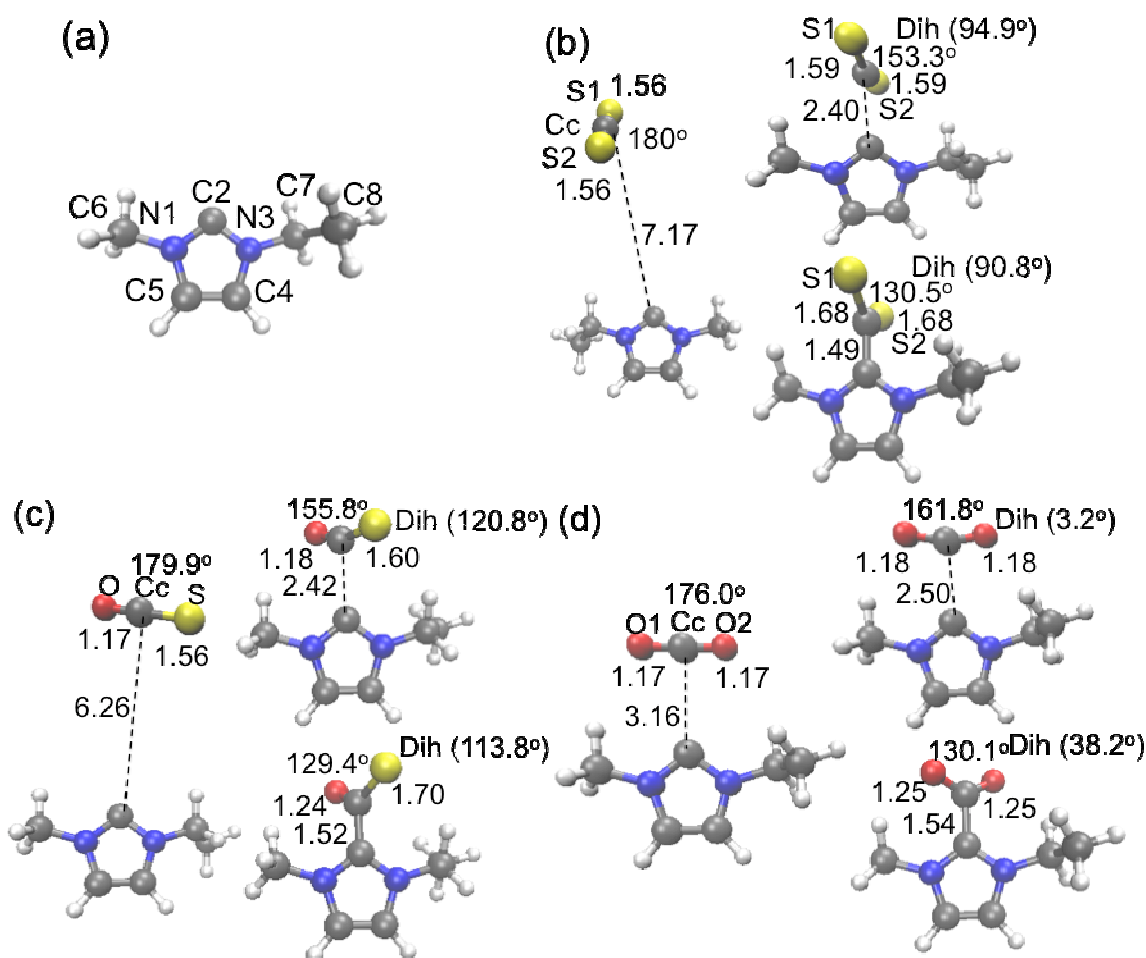
Figure 5. (a) Atom labels for EMI carbene. DFT results for structures of the reactant, product and transition states for direct capture of (b) CS_2, (c) COS, and (d) CO_2 by EMI in the continuum phase (units for distance: Å). Dihedral angle is N-C2-Cc-O(S), between CS_2/COS/CO_2 and the EMI carbene.

Radial distribution functions

Ab initio MD results for radial distribution functions (RDFs) are shown in Figure 6. The distribution of Oa of OAc$^-$ around C2 of EMI$^+$ in Figure 6a exhibits a prominent peak at ~3.0 Å, indicating strong ion pairing between the two. The number of Oa atoms coordinated with C2 determined by integrating this peak is ~2 (Table 2), revealing that virtually all cations and anions are paired with each other in both the pure IL and mixtures.[49] The pronounced peak of the corresponding H2-Oa distribution at ~2 Å indicates that there is a significant interionic hydrogen bonded interaction between C2 and Oa. The integration of the H2-Oa distribution up to 2.4 Å, a typical O-to-H separation employed as an upper bound for intermolecular hydrogen bonds,[79] yields 0.9– 1 (Table 2). This result suggests that nearly all ion pairs form a hydrogen bond between C2 of EMI$^+$ and one of two Oa atoms of OAc$^-$.
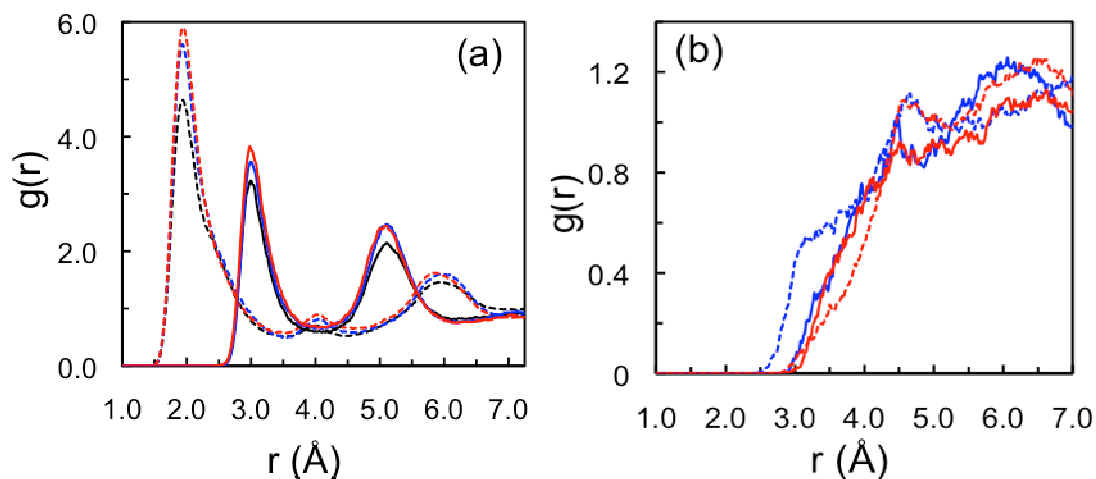
Figure 6. *Ab initio* MD results for radial distribution functions at 298 K. (a) Distributions of C2 (solid) and H2 (dashed) of EMI^+ around Oa of OAc^-. (b) Distributions of Cc of CS_2/COS around C2 (solid) of EMI^+ and Oa (dashed) of OAc^-. The results for the 12:6COS and 12:6CS$_2$ systems are plotted in blue and red, respectively, while those for neat EMI^+OAc^- (12:0) are in black.

The results for COS/CS$_2$ distributions around OAc^-, especially the RDF values in the 2.5–3 Å region, in Figure 6b indicate that COS interacts with OAc^- more strongly than CS$_2$ does. One potential reason is the difference in the Cc charge between COS and CS$_2$, caused by the difference in the electronegativity of O and S. Our DFT calculations predict that in dielectric continuum ($\varepsilon = 15.13$), the partial charge of Cc is 0.357 for COS, while it is -0.016 for CS$_2$. This makes the interaction between Oa and Cc more attractive and therefore stronger for COS than for CS$_2$. By the same token, the Cc-Oa interaction is stronger for CO$_2$ (Cc partial charge = 0.86) than that for COS or CS$_2$ (all partial charges are compiled in Table S3). While the Cc partial charge varies as the separation of Cc and Oa changes due to polarizability, its value in the absence of OAc^- serves as an informative measure to gauge the strength of the electrostatic interaction between the two.

The RDFs of Cc of COS and CS$_2$ around C2 of EMI^+ show a similar behavior; both begin to show structure after 3.0 Å with the first peak around 4.4 Å.

Table 2. *Ab initio* MD results for ion pairing and hydrogen bonds

System	Oa around C2[1)	Hydrogen bonds[2)
12:0	1.93	0.94
12:6COS	1.80	0.94
12:6CS$_2$	1.91	0.96

[1) Number of Oa of acetate in the first solvation shell of C2 of EMI^+.
[2) Number of hydrogen bonds between H2 and Oa per ion pair, obtained by integrating their RDF up to 2.4 Å.[79]

Constrained ab initio MD results for free energetics of CS₂/OCS capture in EMI⁺OAc⁻

Here we consider constrained dynamics *ab initio* MD results to gain quantitative insight into reaction free energetics and mechanisms for CS_2 and COS capture. In ref 49, the same approach was used to investigate CO_2 capture in EMI^+OAc^-.
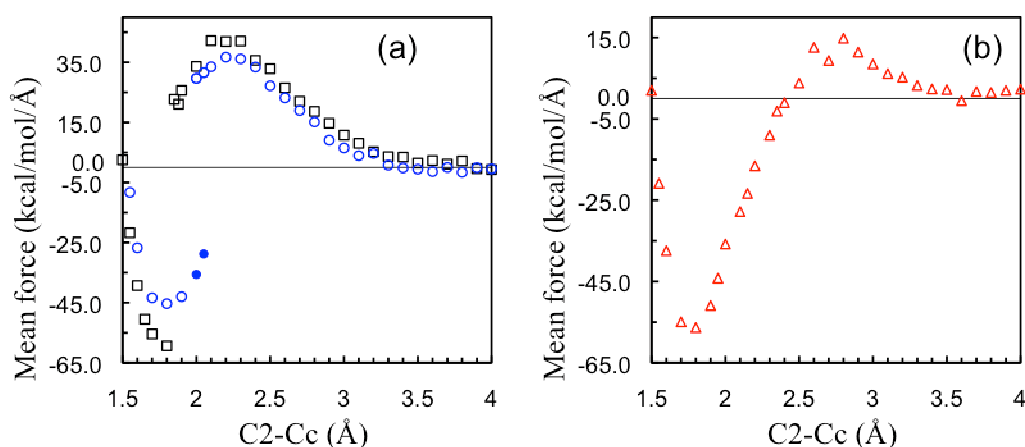

Figure 7. (a) Mean force $f(r)$ between C2 of EMI^+ and Cc of CS_2 (black squares) and Cc of COS (blue circles) in the 12:6CS₂ and 12:6COS systems, respectively; (b) $f(r)$ between C2 of EMI carbene and Cc of CS_2 in 12:6CS₂:1EMI.

The results for the mean force $f(r)$ (eq 1) between C2 of EMI^+ and Cc of CS_2 (black square)/COS (blue circle) are shown as a function of the C2-Cc separation r in Figure 7a. The overall features of $f(r)$ for CS_2 and COS are very similar. The mean force increases as r decreases from ~4 Å, and reaches its maximum around r = 2.1-2.2 Å. As r further decreases, $f(r)$ begins to decrease and then near r = 2 Å, it drops abruptly to a negative value of large magnitude for both CS_2 and COS. This discontinuous change of large amplitude in $f(r)$, which makes the C2-Cc interaction strongly attractive, is due to H2 transfer from EMI^+ to OAc^-. The MD results indicate that the onset of H2 transfer occurs at r = 2.05 Å in the 12:6COS system, whereas it does not occur until r reaches 1.80 Å in the 12:6CS₂ system. This is attributed to the difference in electronegativity of S and O. COS withdraws electron density from EMI^+ better and thus weakens the C2-H2 bond more than CS_2. As a consequence, the rupture of the C2-H2 bond and accompanying transfer of H2 occur earlier, *i.e.*, at larger r in the presence of COS than CS_2. When the constraint on r is removed immediately after H2 transfer, r decreases rapidly and C2 and Cc form a chemical bond nearly instantaneously (result not shown), analogous to the CO_2 capture studied in ref 49. These results strongly suggest that H2 transfer from EMI^+ to OAc^- and carboxylation of EMI^+ by CS_2/COS occur essentially concurrently just like in the CO_2 case.[49] Since EMI carbene is not involved, the concerted mechanism completely bypasses the controversial NHC issues mentioned above.

The activation step in the concerted mechanism is the approach of Cc of CS_2/COS to C2 of EMI^+ in the r region, for which $f(r)$ is positive. By integrating $f(r)$ from the reactant

state to the transition state region, we can estimate the activation free energy. The results for CS_2 and COS are compared in Table 3. The barrier height for CS_2 (33.9 kcal/mol) is much higher than that for COS (21 kcal/mol). One of the main reasons for this big difference is that CS_2 capture is characterized by considerably later transition, *i.e.*, its transition state is located at smaller *r*, than COS capture as noted above. Therefore, all other things being equal, CS_2 needs to do more work to come closer to C2 to reach the transition state than COS does. Additionally, *f(r)* for CS_2 is somewhat larger, *i.e.*, more repulsive, than that for COS. This is ascribed to the difference in the electron withdrawing ability of COS and CS_2 noted above. As Cc approaches C2, COS better facilitates electron density shift[49] from EMI^+ to COS than CS_2 does. As a result, the Cc-C2 interaction is less repulsive for COS than that for CS_2. This also contributes to the difference in activation free energy between the two.

For comparison, we have examined *f(r)* for the direct capture of CS_2 by NHC, *i.e.*, EMI carbene, in the 12IP:6CS$_2$:1EMI system (Figure 7b). It should be noted that in the continuum limit, the 12IP:6CS$_2$:1EMI system becomes similar to that used in the *ab initio* SCRF analysis in Figure 5b above. In contrast to the concerted pathway in Figure 7a, *f(r)* for the direct capture behaves smoothly in the entire *r* region we studied. The maximum of *w(r)*, characterized by *f(r)* = 0 and *df(r)/dr* > 0, which we identify as the transition state for the direct capture, is located at *r* = ~2.4 Å in excellent agreement with the *ab initio* SCRF result in Figure 5b. The activation free energy obtained by the integration of *f(r)* is 12.5 kcal/mol, which also compares very well with the *ab initio* SCRF result 13.3 kcal/mol in Table 1. This indicates that our *ab initio* SCRF and *ab initio* MD results are consistent and thus robust.

Table 3 Energy barrier E_a along the C2–Cc coordinate and activation free energy (units: kcal/mol)

System	r_{pt} [1]	E_a [2]	Activation free energy [3]
12:6CO$_2$ [4]	2.10 Å	23.5	20.0
12:6COS	2.05 Å	24.5	21.0
12:6CS$_2$	1.80 Å	37.4	33.9
12:6CS$_2$:1EMI	–	12.5	12.5 (no ZPE)

[1] Maximum Cc-C2 distance at which H2 transfer from EMI^+ to OAc^- occurs.
[2] Calculated as the integration of *f(r)* from 4.0 Å to r_{pt}.
[3] Determined as the difference of E_a and the zero-point energy (ZPE) of C2-H2 stretching vibration of EMI^+.
[4] From ref 49.

Important mechanistic insights into CS_2/COS capture processes can now be gained by the comparison of free energetics of conversion and direct capture reactions. If the capture proceeds in a concerted fashion, the barrier height for CS_2 capture (33.9 kcal/mol) is much higher than that for conversion of CS_2 to COS (21.4 kcal/mol). This means that virtually all CS_2 will be converted to COS through S/O exchange with OAc^- before it can be captured by EMI^+OAc^-. This provides an excellent theoretical explanation for the aforementioned experimental finding[56,57] that the 1-alkyl-3-methylimidazole-2-

dithiocarboxylate species is not produced in the CS$_2$ reaction system. Activation barriers for COS capture (21 kcal/mol) and COS conversion to CO$_2$ (20.4 kcal/mol), on the other hand, are nearly the same. Therefore both capture and conversion reactions will occur for COS, and (part of) CO$_2$ produced via the conversion of COS will be captured subsequently by the IL. Thus, the concerted mechanism predicts that both 1-alkyl-3-methylimidazole-2-thiocarboxylate and 1-alkyl-3-methylimidazole-2-carboxylate will be formed as the reaction product but not 1-alkyl-3-methylimidazole-2-dithiocarboxylate, in perfect agreement with the measurements. Furthermore, conclusions drawn based on this comparison By contrast, the activation barrier for direct capture of CS$_2$ by EMI carbene is about 13 kcal/mol, which is much lower than the barrier height 20.4 kcal/mol for its conversion to COS. Therefore, if NHC would be indeed pre-formed in the imidazolium acetate IL, it would capture CS$_2$ and form 1-alkyl-3-methylimidazole-2-dithiocarboxylate, prior to the conversion of CS$_2$ to COS! Near complete absence of the dithiocarboxylate compound observed in experiments rules out the direct capture mechanism, providing strong evidence that NHC is not formed in imidazolium acetate.

As indicated above, several key conclusions of our work are based on direct comparison of the SCRF and *ab initio* MD results—specifically, the former for CS$_2$ and COS conversion in EMI$^+$OAc$^-$ and the latter for their capture by the IL. While care should be taken in such a comparison, we nevertheless think that the solvation effect is accounted for at the quantitative level in our SCRF calculations as rationalized above and therefore our comparative analysis is solid. This is further justified by the excellent agreement noted above between our theoretical findings and available experimental information[56,57] on reaction pathways and kinetics of the CS$_2$-EMI$^+$OAc$^-$ mixture.

Conclusions

In this article, we have studied possible reaction pathways for CS$_2$ and COS in the ionic liquid, EMI$^+$OAc$^-$. These included conversion of CS$_2$ to COS and COS to CO$_2$ via S/O exchange with OAc$^-$ as well as their capture by the IL which will produce EMI-CS$_2$ and EMI-COS, respectively. One of the main highlights of our work is that the capture reaction, if allowed, occurs in a concerted fashion and thus N-heterocyclic carbene species—which has been the subject of recent controversy—is not involved throughout the entire reaction process. For CS$_2$, the barrier height for the capture is much higher than that for the conversion and as a result, its reaction proceeds almost exclusively along the conversion pathway. By contrast, the barrier heights for the capture and the conversion of COS are nearly the same, so that both reactions take place. These results are in perfect agreement with recent experimental findings.[56,57]

Another important finding is that if NHC would be present in the imidazolium acetate ionic liquids, it would react with CS$_2$ and form 1-ethyl-3-methylimidazole-2-dithiocarboxylate, EMI-CS$_2$, prior to the CS$_2$-to-COS conversion. This result, combined with the experimentally-observed absence of the imidazole-2-dithiocarboxylate compound in real reaction systems,[56,57] lends support to the view that NHC is not formed in the imidazalium acetate ionic liquids.[49] One noteworthy consequence of this is that if

the formation of NHC can be induced in imidazolium acetate, *e.g.*, by the addition of a strong base, imidazole-2-dithiocarboxylate species would be generated as the product of the capture of CS_2. It would thus be interesting to see if this prediction is borne out experimentally because it not only provides additional insight on the CS_2 reaction mechanisms in imidazolium acetate but also casts illuminating light on controversial NHC in this ionic liquid family.

Supplementary Information

Optimized structures of $CS_2/COS/CO_2$ and EMI carbene in the gas and continuum phases, optimized structures of the reactant, product, intermediate and transition states for the conversion of CS_2/COS to $COS/CO2$ and their capture by EMI, comparison of SCRF results for COS-to-CO_2 conversion in 1-pentanol and in ethanol, electric dipole moments of the reactant, product and transition states for capture of CS_2, COS and CO_2 by EMI carbene, and partial charges for $CS_2/COS/CO_2$ and Cc atom of EMI carbene.

Acknowledgments

REFERENCES

[1].   T. Welton, *Room-Temperature Ionic Liquids. Solvents for Synthesis and Catalysis*, Chem. Rev. **1999**, *99*, 2071-2083.

[2].   C. Chiappe and D. Pieraccini*, Ionic liquids: solvent properties and organic reactivity*, J. Phys. Org. Chem. **2005**, *18*, 275–297. □

[3].   F. Endres and S. Z. E. Abedin, *Air and Water Stable Ionic Liquids in Physical Chemistry*, Phys. Chem. Chem. Phys. **2006**, *8*, 2101–2116.

[4].   J. Dupont and P. A. Z. Suarez, *Physico-Chemical Processes in Imidazolium Ionic Liquids*, Phys. Chem. Chem. Phys. **2006**, *8*, 2441–2452.

[5].   K. R. Seddon, *Ionic Liquids for Clean Technology*, J. Chem. Technol. Biotechnol. **1997**, *68*, 351-356.

[6].   J. G. Huddleston, H. W. Willauer, R. P. Swatloski, A. E. Visser, and R. D. Rogers, *Room temperature ionic liquids as novel media for 'clean' liquid–liquid extraction*, Chem. Commun. **1998,** *16*, 1765-1766.

[7].   M. J. Earle and K. R. Seddon, *Ionic Liquids. Green Solvents for the Future*, Pure Appl. Chem. **2000**, *72*, 1391–1398.

[8].   P. Wasserscheid and W. Keim, *Ionic Liquids-New "Solutions" for Transition Metal Catalysis*, Angew. Chem. Int. Ed. **2000**, *39*, 3772–3789.

[9].   P. G. Jessop, C. A. Eckert, C. L. Liotta, R. J. Bonilla, J. S. Brown, R. A. Brown, P. Pollet, C. A. Thomas, C. Wheeler and D. Wynne, *Catalysis Using Supercritical or Subcritical Inert Gases Under Split-Phase Conditions, in Clean Solvents*, edited by L. Moens and M. A. Abraham, ACS, Washington, DC, 2002.

[10].   T. Welton, *Ionic Liquids in Green Chemistry*, Green Chem. **2001**, *13*, 225–225.

[11].   N. V. Plechkova and K. R. Seddon, *Applications of Ionic Liquids in the Chemical Industry*, Chem. Soc. Rev. **2008**, *37*, 123–150.

[12].   F. V. Rantwijk and R. A. Sheldon, *Biocatalysis in Ionic Liquids*, Chem. Rev. **2007**, *107*, 2757–2785.

[13].   Z. C. Zhang, *Catalysis in Ionic Liquids*, Adv. Catal. **2006**, *49*, 153–237.

[14].   S. M. A. De Wildeman, T. Sonke, H. E. Schoemaker and O. May, *Biocatalytic Reductions: From Lab Curiosity to First Choice*, Acc. Chem. Res., **2007**, *40*, 1260-1266.

[15].   P. S. Kulkarni, L. C. Branco, J. G. Crespo and C. A. M. Afonso, *Capture of Dioxins by Ionic Liquids*, Environ. Sci. Tech. **2008**, *42*, 2570–2574.

[16].   C. Zhang, K. Huang, P. Yu, H. Liu, *Ionic liquid based three-liquid-phase partitioning and one-step separation of Pt(IV), Pd(II) and Rh(III)*, Sep. Purif. Technol. **2013**, 108, 166–173.

[17].   J. Park, Y. Jung, P. Kusumah, J. Lee, K. Kwon and C. K. Lee, *Application of Ionic Liquids in Hydrometallurgy*, Int. J. Mol. Sci. **2014**, *15*, 15320–15343.

[18].   M. Armand, F. Endres, Frank D. R. MacFarlane, H. Ohno, and B. Scrosati, *Ionic-liquid materials for the electrochemical challenges of the future,* Nat. Mater. **2009**, *8,* 621–629.

[19].   J. F. Brennecke and B. E. Gurkan, *Ionic Liquids for CO_2 Capture and Emission Reduction*, J. Phys. Chem. Lett. **2010**, *1*, 3459–3464.

[20].   M. B. Shiflett, D. W. Drew, R. A. Cantini and A. Yokozeki, *Carbon Dioxide Capture Using Ionic Liquid 1-Butyl-3-methylimidazolium Acetate*, Energy Fuels **2010**, *24*, 5781–5789.

[21].   X. Zhang, X. Zhang, H. Dong, Z. Zhao, S. Zhang, Y. Huang, *Carbon capture with ionic liquids: overview and progress*, Energy Environ. Sci.*, **2012**, *5*, 6668–6681.

[22].   A. Bosmann, L. Datsevich, A. Jess, A. Lauter, C. Schmitz, and P. Wasserscheid, *Deep desulfurization of diesel fuel by extraction with ionic liquids*, Chem. Comm. **2001**, 2494–2495.

[23].   C. Huang, B. Chen, J. Zhang, Z. Liu, and Y. Li, *Desulfurization of Gasoline by Extraction with New Ionic Liquid*, Energy Fuels **2004**, 18, 1862–1864.

[24].   R. P. Swatloski, S. K. Spear, J. D. Holbrey and R. D. Rogers, *Dissolution of Cellulose with Ionic Liquids*, J. Am. Chem. Soc. **2002**, *124*, 4974–4975.

[25].   A. Pinkert, K. N. Marsh, S. Pang and M. P. Staiger, *Ionic Liquids and Their Interaction with Cellulose,* Chem. Rev. **2009**, *109*, 6712–6728.

[26].   H. Tadesse and R. Luque, *Advances on Biomass Pretreatment Using Ionic Liquids: An Overview*, Energy Environ. Sci. **2011**, *4*, 3913–3929.

[27].   M. Gericke, P. Fardim and T. Heinze, *Ionic Liquids — Promising but Challenging Solvents for Homogeneous Derivatization of Cellulose*, Molecules **2012**, *17*, 7458–7502.

[28].   Kosuke Kuroda, Heri Satria, Kyohei Miyamura, Kazuaki Ninomiya, Kenji Takahashi, *Design of Wall-Destructive but Membrane-Compatible Solvents*, J. Am. Chem. Soc. **2017**, 139(45), 16052-16055.

[29].   Takatsugu Endo Ei Mon Aung, Shunsuke Fujii, Shota Hosomi, Mitsugu Kimizu, Kazuaki Ninomiya, Kenji Takahashi, *Investigation of accessibility and reactivity*

of cellulose pretreated by ionic liquid at high loading, Carbohydrate Polymers, **2017**, 176, 365-373.

[30]. Takatsugu Endo, Shota Hosomi, Shunsuke Fujii, Kazuaki Ninomiya, Kenji Takahashi, *Anion Bridging-Induced Structural Transformation of Cellulose Dissolved in Ionic Liquid*, J. Phys. Chem. Lett. **2016**, 7(24), 5156-5161).

[31]. M. Lazzari, C. Arbizzani, F. Soavi, and M. Mastragostino, *EDLCs Based on Solvent-Free Ionic Liquids, in Supercapacitors: Materials, Systems, and Applications*, edited by F. Beguin and E. Frackowiak, Wiley-VCH, 2013.

[32]. M. Egashira, H. Todo, N. Yoshimoto and M. Morita, *Lithium ion conduction in ionic liquid-based gel polymer electrolyte*, J. Power Sources **2008**, *178*, 729-735.

[33]. L. Lombardo, S. Brutti, M. A. Navarra, S. Panero, P. Reale, *Mixtures of ionic liquid – Alkylcarbonates as electrolytes for safe lithium-ion batteries*, J. Power Sources **2013**, *227*, 8–14.

[34]. M. Kar, T. J. Simons, M. Forsyth, and D. R. MacFarlane, *Ionic liquid electrolytes as a platform for rechargeable metal-air batteries: a perspective,* Phys. Chem. Chem. Phys. **2014***, 16,* 18658–18674.

[35]. F. Hao and H. Lin, *Recent molecular engineering of room temperature ionic liquid electrolytes for mesoscopic dye-sensitized solar cells*, RSC Adv. **2013**, *3*, 23521–23532.

[36]. H. Rodríguez, G. Gurau, J. D. Holbrey and R. D. Rogers, *Reaction of elemental chalcogens with imidazolium acetates to yield imidazole-2-chalcogenones: direct evidence for ionic liquids as proto-carbenes*, Chem. Commun. **2011**, *47*, 3222–3224.

[37]. Z. Kelemen, O. Hollóczki, J. Nagy and L.Nyulászi, *An organocatalytic ionic liquid*, Org. Biomol. Chem. **2011**, *9*, 5362–5364.

[38]. D. J. Liu, Y. Zhang and E. Y.-X. Chen, *Organocatalytic upgrading of the key biorefining building block by a catalytic ionic liquid and N-heterocyclic carbenes*, Green Chem. **2012**, *14*, 2738–2746.

[39]. I. Chiarotto, M. Feroci and A. Inesi, *First direct evidence of N-heterocyclic carbene in BMIm acetate ionic liquids. An electrochemical and chemical study on the role of temperature*, New J. Chem. **2017**, *41*, 7840–7843.

[40]. N. M. A. N. Daud, E. Bakis, J. Hallett, C. C. Weber and T. Welton*, Evidence for the spontaneous formation of N-heterocyclic carbenes in imidazolium based ionic liquids*, Chem. Commun. **2017**, *53*, 11154–11156.

[41]. E. J. Maginn, *Design and evaluation of ionic liquids as novel CO_2 absorbents. Quarterly Technical Report to DOE*, 2005.

[42]. G. Gurau, H. Rodríguez, S. P. Kelley, P. Janiczek, R. S. Kalb and R. D. Rogers, *Demonstration of Chemisorption of Carbon Dioxide in 1,3-Dialkylimidazolium Acetate Ionic Liquids*, Angew. Chem., Int. Ed. **2011**, *50*, 12024–12026.

[43]. M. Besnard, M. I. Cabaço, F. V. Chávez, N. Pinaud, P. J. Sebastião, J. A. P. Coutinho and Y. Danten, *On the spontaneous carboxylation of 1-butyl-3-methylimidazolium acetate by carbon dioxide*, Chem. Commun. **2012**, *48*, 1245–1247.

[44]. M. I. Cabaço, M. Besnard, Y. Danten and J. A. P. Coutinho, *Carbon Dioxide in 1-Butyl-3-methylimidazolium Acetate. I. Unusual Solubility Investigated by Raman Spectroscopy and DFT Calculations*, J. Phys. Chem. A, **2012**, *116*, 1605–1620.

[45]. M. Besnard, M. I. Cabaço, F. V. Chávez, N. Pinaud, P. J. Sebastião, J. A. P. Coutinho, J. Mascetti and Y. Danten, *CO$_2$ in 1-Butyl-3-methylimidazolium Acetate. 2. NMR Investigation of Chemical Reactions*, J. Phys. Chem. A, **2012**, *116*, 4890–4901.

[46]. W. Shi, C. R. Meyers, D. R. Luebke, J. A. Steckel, D. C. Sorescu, *Theoretical and Experimental Studies of CO$_2$ and H$_2$ Separation Using the 1-Ethyl-3-methylimidazolium Acetate ([Emim][CH$_3$COO]) Ionic Liquid*, J. Phys. Chem. B **2012**, *116*, 283–295.

[47]. O. Hollóczki, D. S. Firaha, J. Friedrich, M. Brehm, R. Cybik, M. Wild, A. Stark, B. Kirchner, *Carbene Formation in Ionic Liquids: Spontaneous, Induced, or Prohibited?* J. Phys. Chem. B*, **2013**, *117*, 5898-5907.

[48]. J. X. Mao, J. A. Steckel, F. Yan, N. R. Dhumal, D. R. Luebke, H. J. Kim, K. Damodaran, *Understanding the mechanism of CO$_2$ capture by 1,3 di-substituted imidazolium acetate based ionic liquids*, Phys. Chem. Chem. Phys. **2016**, *18*, 1911–1917.

[49]. F. Yan, N. R. Dhumal and H. J. Kim, *CO$_2$ capture in ionic liquid 1-alkyl-3-methylimidazolium acetate: A concerted mechanism without carbene*, Phys. Chem. Chem. Phys. **2017**, *19*, 1361–1368.

[50]. R. Kakuchi, R. Ito, S. Nomura, H. Abroshan, K. Ninomiya, T. Ikai, K. Maeda, H. J. Kim and K. Takahashi, *A mechanistic insight into organocatalytic properties of imidazolium-based ionic liquids and a positive co-solvent effect on cellulose modification reactions in an ionic liquid*, RSC Adv. **2017**, *7*, 9423–9430; *Correctio*n, RSC Adv. **2017**, *7*, 13876.

[51]. Eric M. Simmons and John F. Hartwig, *On the Interpretation of Deuterium Kinetic Isotope Effects in C H Bond Functionalizations by Transition- Metal Complexes□*, Angew. Chem. Int. Ed. **2012**, 51, 3066 – 3072.

[52]. D. Enders, O. Niemeier and A. Henseler, *Organocatalysis by N-heterocyclic carbenes*, Chem. Rev., 2007, **107**, 5606-5655.

[53]. W. A. Herrmann, *N-Heterocyclic Carbenes: A New Concept in Organometallic Catalysis*, Angew. Chem. Int. Ed., 2002, **41**, 1290-1309.

[54]. W. A. Herrmann, M. Elison, J. Fischer, C. Köcher and G. R. J. Artus, *N-Heterocyclic Carbened$^{[+]}$: Generation under Mild Conditions and Formation of Group 8-10 Transition Metal Complexes Relevant to Catalysis*, Chem. Eur. J. **1996** , *2*, 772–780.

[55]. F. E. Hahn and M. C. Jahnke, *Heterocyclic Carbenes: Synthesis and Coordination Chemistry*, Angew. Chem. Int. Ed. **2008**, *47*, 3122 – 3172.

[56]. M. I. Cabaço, M. Besnard, F. V. Chávez, N. Pinaud, P. J. Sebastião, J. A. P. Coutinho, J. Mascetti and Y. Danten, *On the chemical reactions of carbon dioxide isoelectronic molecules CS$_2$ and OCS with 1-butyl-3-methylimidazolium acetate*, Chem. Commun. **2013**, *49*, 11083–11085.

[57]. M. I. Cabaço, M. Besnard, F. V. Chávez, N. Pinaud, P. J. Sebastião, J. A. P. Coutinho, and Y. Danten, *Understanding chemical reactions of CO$_2$ and its isoelectronic molecules with 1-butyl-3-methylimidazolium acetate by changing the nature of the cation: The case of CS$_2$ in 1-butyl-1-methylpyrrolidinium acetate studied by NMR spectroscopy and density functional theory calculations*, J. Chem. Phys*, **2014**, *140*, 244307.

[58]. Y. Danten, M. I. Cabaço, J. A. P. Coutinho, N. Pinaud, and M. Besnard, *DFT Study of the Reaction Mechanisms of Carbon Dioxide and its Isoelectronic Molecules CS$_2$ and OCS Dissolved in Pyrrolidinium and Imidazolium Acetate Ionic Liquids*, J. Phys. Chem. B **2016**, *120*, 5243−5254.

[59]. M. J. Frisch, G. W. Trucks, H. B. Schlegel, G. E. Scuseria, M. A. Robb, J. R. Cheeseman, J. A. Montgomery, Jr. T. Vreven, K. N. Kudin, J. C. Burant, J. M. Millam, S. S. Iyengar, J. Tomasi, V. Barone, B. Mennucci, M. Cossi, G. Scalmani, N. Rega, G. A. Petersson, H. Nakatsuji, M. Hada, M. Ehara, K. Toyota, R. Fukuda, J. Hasegawa, M. Ishida, T. Nakajima, Y. Honda, O. Kitao, H. Nakai, M. Klene, X. Li, J. E. Knox, H. P. Hratchian, J. B. Cross, C. Adamo, J. Jaramillo, R. Gomperts, R. E. Stratmann, O. Yazyev, A. J. Austin, R. Cammi, C. Pomelli, J. W. Ochterski, P. Y. Ayala, K. Morokuma, G. A. Voth, P. Salvador, J. J. Dannenberg, V. G. Zakrzewski, S. Dapprich, A. D. Daniels, M. C. Strain, O. Farkas, D. K. Malick, A. D. Rabuck, K. Raghavachari, J. B. Foresman, J. V. Ortiz, Q. Cui, A. G. Baboul, S. Clifford, J. Cioslowski, B. B. Stefanov, G. Liu, A. Liashenko, P. Piskorz, I. Komaromi, R. L. Martin, D. J. Fox, T. Keith, M. A. Al-Laham, C. Y. Peng, A. Nanayakkara, M. Challacombe, P. M. W. Gill, B. Johnson, W. Chen, M. W. Wong, C. Gonzalez, J. A. Pople, *Gaussion 03, Gaussian, Inc., Wallingford CT*, 2004.

[60]. A. D. Becke, *Density-functional thermochemistry. III. The role of exact exchange,* J. Chem. Phys. **1993**, *98***,** 5648-52.

[61]. C. Lee, W. Yang, R. G. Parr, *Development of the Colle-Salvetti correlation-energy formula into a functional of the electron density*, Phys. Rev. B **1988**, *37***,** 785-789.

[62]. Y. Zhao and D. G. Truhlar, *The M06 suite of density functionals for main group thermochemistry, thermochemical kinetics, noncovalent interactions, excited states, and transition elements: two new functionals and systematic testing of four M06-class functionals and 12 other functionals*, Theor. Chem. Acc. **2008**, *120*, 215-241.

[63]. J. Hutter, M. Iannuzzi, F. Schiffmann and J. VandeVondele, *cp2k: atomistic simulations of condensed matter systems,* Comput. Mol. Sci. **2014**, *4*, 15–25.

[64]. S. Pronk, S. Páll, R. Schulz, P. Larsson, P. Bjelkmar, R. Apostolov, M. R. Shirts, J. C. Smith, P. M. Kasson, D. van der Spoel, B. Hess and E. Lindahl, *GROMACS 4.5: a high-throughput and highly parallel open source molecular simulation toolkit.* Bioinformatics, **2013**, *29*, 845–854.

[65]. M. S. Kelkar, W. Shi and E. J. Maginn, *Determining the Accuracy of Classical Force Fields for Ionic Liquids: Atomistic Simulation of the Thermodynamic and Transport Properties of 1-Ethyl-3-methylimidazolium Ethylsulfate ([emim][EtSO4]) and Its Mixtures with Water*, Ind. Eng. Chem. Res. **2008**, *47*, 9115–9126.

[66]. W. Shi, C. R. Meyers, D. R. Luebke, J. A. Steckel and D. C. Sorescu, *Theoretical and experimental studies of CO2 and H2 separation using the 1-ethyl-3-methylimidazolium acetate ([emim][CH3COO]) ionic liquid*, J. Phys. Chem. B **2012**, *116*, 283–295.

[67]. H. Torii, *The role of atomic quadrupoles in intermolecular electrostatic interactions of polar and nonpolar molecules*, J. Chem. Phys. **2003**, *119*, 2192-2198.

[68]. D. J. Tildesley, P. A. Madden, *An effective pair potential for liquid carbon disulphide*, Mol. Phys. **1981**, *42*, 1137-1156.

[69]. A. A. Deakin, S. H. Walmsley, *Potential functions and the lattice dynamics of carbonyl sulphide,* Chem. Phys. **1989**, *136*, 105-113.

[70]. C. M. Breneman, K. B. Wiberg, *Determining atom‐centered monopoles from molecular electrostatic potentials. The need for high sampling density in formamide conformational analysis*, J. Comput. Chem. **1990**, *11*, 361-373.

[71]. A. D. Becke, *Density-functional exchange-energy approximation with correct asymptotic behavior*. Phys. Rev. A **1988**, *38*, 3098–3100.

[72]. S. Grimme, *Semiempirical GGA-type density functional constructed with a long-range dispersion correction*, J. Comput. Chem. **2006**, *27*, 1787–1799.

[73]. S. Goedecker, M. Teter and J. Hutter, *Separable dual-space Gaussian pseudopotentials*. Phys. Rev. B, **1996**, *54*, 1703–1710.

[74]. S. Nosé, *A unified formulation of the constant temperature molecular dynamics methods*, J. Chem. Phys. **1984**, *81*, 511–519.

[75]. W. G. Hoover, *Canonical dynamics: Equilibrium phase-space distributions*, Phys. Rev. A, **1985**, *31*, 1695–1697.

[76]. For an extensive list of experimental and theoretical studies of effective polarity of ILs, see E. Wu, H. J. Kim, *MD Study of Stokes Shifts in Ionic Liquids: Temperature Dependence*, J. Phys. Chem. B, **2016**, *120*, 4644–4653.

[77]. Y. Shim, M. Y. Choi and H. J. Kim, *A Molecular Dynamics Computer Simulation Study of Room-Temperature Ionic Liquids. I. Equilibrium Solvation Structure and Free Energetics,* J. Chem. Phys. **2005**, *122*, 044510.

[78]. Y. Shim, D. Jeong, S. R. Manjari, M. Y. Choi, and H. J. Kim, *Solvation, Solute Rotation and Vibration Relaxation, and Electron Transfer Reactions in Room-Temperature Ionic Liquids,* Acc. Chem. Res. **2007**, *40*, 1130–1137.

[79]. B. D. Bursulaya, H. J. Kim, *Molecular dynamics simulation study of water near critical conditions. I. Structure and solvation free energetics,* J. Chem. Phys., **1999**, *110*, 9646-9655 and references therein.